Conformational Analysis of Poly(alkoxy- and aryloxyphosphazenes)[1,2]

Robert W. Allen and Harry R. Allcock*

Department of Chemistry, The Pennsylvania State University, University Park, Pennsylvania 16802. *Received March 8, 1976*

ABSTRACT: The poly(organophosphazenes), $[NP(OCH_3)_2]_n$, $[NP(OCH_2CH_3)_2]_n$, $[NP(OCH_2CF_3)_2]_n$, and $[NP(OC_6H_5)_2]_n$, have been studied by conformational analysis techniques with the use of intramolecular nonbonding 6:12 Lennard-Jones and Coulombic potentials. The energy surfaces reveal broad areas of low potential for the methoxy, ethoxy, and trifluoroethoxy derivatives that are consistent with the very low glass transition temperatures and a high chain mobility. Backbone torsional motions appear to be more restricted for the phenoxy derivative and this is compatible with a higher T_g value. Low potential energy wells are found at points which correspond to the approximately cis-trans conformation inferred from x-ray diffraction data from $[NP(OCH_2CF_3)_2]_n$ and $[NP(OC_6H_5)_2]_n$.

The synthesis of high molecular weight poly(alkoxy- and aryloxyphosphazenes) (I) has been described in earlier pub-

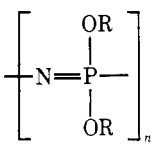

I

lications.[3-5] A substantial number of polymers of this type are now known which contain different alkoxy or aryloxy substituents either as homopolymers or as mixed-substituent derivatives.[6-10] The introduction of different substituents generates markedly different properties, and polymers are known which range from low temperature elastomers[5,11,12] to high melting, crystalline thermoplastics.[3,4] This synthetic versatility of phosphazenes is perhaps their most unusual and valuable attribute.

The synthetic work has revealed the fact that some polyphosphazenes exhibit very low glass transition temperatures (T_g). For example, poly(difluorophosphazene), $(NPF_2)_n$, has a T_g value near −95 °C,[13] and poly(dichlorophosphazene), $(NPCl_2)_n$, has a T_g near −66 °C.[4,14] These values are indicative of an unusually high degree of backbone torsional mobility that is perhaps unexpected for an inorganic polymer system. The preceding paper[15] has analyzed this behavior in terms of the broad, low-energy plateaus that exist in the conformational energy surfaces of the fluoro and chloro derivatives.

However, it is also known that the replacement of chlorine atoms in $(NPCl_2)_n$ by specific alkoxy groups either lowers the T_g or leaves it virtually unchanged. For example, $[NP(OCH_3)_2]_n$ has a T_g value near −76 °C,[4] $[NP(OCH_2CH_3)_2]_n$ has a value near −84 °C,[4] and $[NP(OCH_2CF_3)_2]_n$ has a T_g in the −66 to −53 °C region.[4,14] The ethoxy and trifluoroethoxy groups are bulky substituents and their presence might have been expected to inhibit the torsional motions of the backbone bonds. The introduction of a pentafluoropropyl group in $[NP(OCH_2CF_2CF_3)_2]_n$ or a phenoxy group in $[NP(OC_6H_5)_2]_n$[4] raises the T_g to −25 and −8 °C, respectively.

Intuitively, it can be postulated that the torsional freedom of the backbone bonds may be largely unaffected by the presence of bulky substituent groups if these groups themselves have the conformational mobility needed to avoid serious intramolecular repulsions. The present work was designed to explore this possibility. An additional purpose of this study was to search for conformational energy minima that might be correlated with chain conformations deduced from x-ray diffraction data. The four polymers analyzed in this work were $[NP(OCH_3)_2]_n$, $[NP(OCH_2CH_3)_2]_n$, $[NP(OCH_2CF_3)_2]_n$, and $[NP(OC_6H_5)_2]_n$.

Models and Method

The Models. The structures shown in II–V were employed to generate energy surfaces for the four polymers. Because of the complexity of all four systems, the following assumptions and approximations were made:

(1) It was assumed that the conformational behavior of a long chain can be simulated by the behavior of a short segment that contains only five-skeletal atoms. It was recognized that the use of a longer chain segment would have been preferred,

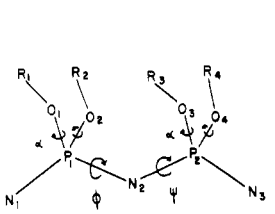

II

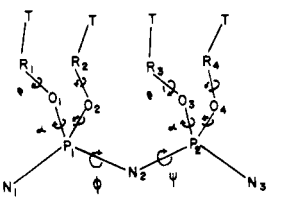

III

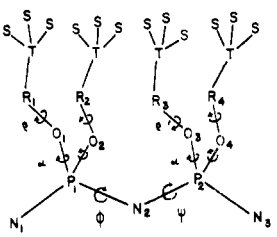

IV

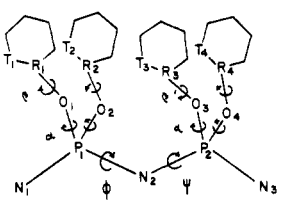

V

but an investigation of longer model segments was precluded by the limits of the available computational system. Moreover, it had previously been shown[2] that only minor differences existed between the surfaces when a five-skeletal atom unit was compared with a seven-skeletal atom section for simpler polymers, such as $(NPF_2)_n$, $(NPCl_2)_n$, or $(NPBr_2)_n$.

(2) Skeletal torsional motions about bonds P_1–N_2 (ϕ) and N_2–P_2 (ψ) were performed in 10° increments.

(3) A threefold rotational model was employed for torsion of the P–O bonds (α). The staggered conformations depicted in VI were used (the view in VI is down the P_1–O_1 bond). It should be noted that, because the disposition of bonds around

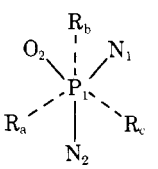

VI

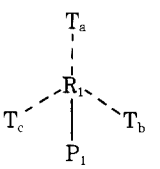

VII

Table I
Bond Angles and Bond Lengths Used in the Different Models

	$[NP(OCH_3)_2]_n$–A[a]	$[NP(OCH_3)_2]_n$–B[b]	$[NPOCH_2CH_3)_2]_n$	$[NP(OCH_2CF_3)_2]_n$	$[NP(OC_6H_5)_2]_n$[e]
PN, Å	1.56	1.56	1.56[b]	1.56[b]	1.56[f]
PO, Å	1.58	1.58	1.56[c]	1.56[c]	1.58
OC, Å	1.42	1.44	1.45[c]	1.45[c]	1.41
CC, Å			1.45[c]	1.45[c]	1.37
CH, Å			1.0		
CF, Å				1.34[d]	
NPN, deg	121.0	116.7	117[b]	117[b]	117.3
PNP, deg	130[g]	130[g]	130[g]	130[g]	130[g]
POC, deg	121.0	120.6	122[c]	122[c]	123.2
OPO, deg	105.5	101.3	100[b]	100[b]	100.1
OCC, deg			109.2	109.2[c]	120
CCH, deg			109.5		
CCF, deg				110[d]	

[a] From $[NP(OCH_3)_2]_4$.[25] [b] From $[NP(OCH_3)_2]_8$.[26] [c] From $MgP(OCH_2CH_3)O_2$.[18] [d] From CF_3CH_2OH.[29] [e] From $[NP(OC_6H_5)_2]_3$.[30] [f] Shortened from 1.58 Å, as observed in higher cyclic and polymeric phosphazenes. [g] All the P–N–P angles were fixed at 130°, a value estimated from earlier work.[2]

phosphorus is not strictly tetrahedral, the coordinate transfers were made to bisect the N_1–P–N_2 angle or the N–P–O_2 angles. For models III–V, additional threefold rotation was allowed about the O–R bonds (β). The conformations considered are shown in VII (the view in VII is down the O–R bond).

(4) For model II (used for $[NP(OCH_3)_2]_n$), the methyl group was treated as an enlarged carbon atom according to the method of Gibson and Scheraga.[15]

(5) The polymer, $[NP(OCH_2CH_3)_2]_n$, was treated with the use of models III and IV. When model III was employed, the methyl and methylene units were considered as individual "atoms".[15] When model IV was used for this polymer, the methyl hydrogen atoms were considered individually, with the methyl group arrayed in a staggered conformation, relative to the C–O bond.

(6) The trifluoroethoxy derivative, $[NP(OCH_2CF_3)_2]_n$, was examined with the use of structure IV, in which individual fluorine atoms were introduced, with a staggered conformation assumed for the trifluoromethyl unit.

(7) Poly(diphenoxyphosphazene), $[NP(OC_6H_5)_2]_n$, was treated by the use of structure V. Hydrogen atoms were not incorporated into the model, but "expanded carbon atoms" were utilized in the phenyl residues.[16]

In all four structures, the initial position ($\psi = 0$, $\phi = 0$) was the trans-trans planar backbone conformation depicted in II–V. For *each* backbone conformation, 81 possible conformations (rotation α) exist for the side group units in II and 6561 possibilities (rotation α and β) for III–V. Hence, as described below, the side group conformations were allowed to undergo energy minimization at each backbone conformation before calculation of the final total interaction energy.

The choice of interatomic distances and bond angles (Table I) was based parly on x-ray crystallographic data obtained from cyclic phosphazene oligomers.[17] Parameters for the ethoxy and trifluoroethoxy side groups were estimated from the appropriate phosphate ester crystallographic data.[18] The most critical parameter in the model is the choice of a P–N–P skeletal bond angle. Earlier observations[19] and calculations[2] had shown that this angle can respond to the constraints of a cyclic six- or eight-membered ring. Hence, the values obtained from structural work on small-ring cyclic oligomers cannot be used directly for the high polymers. The value of 130°, chosen for all four polymers, was based on the known x-ray diffraction repeat distances for several phosphazene polymers and the results of conformational calculation work for polymers, such as $(NPF_2)_n$, $(NPCl_2)_n$, and $(NPBr_2)_n$.[15]

Potential Energy Calculations. The conformational analysis was carried out with the use of a Lennard–Jones "6:12" potential of the form, $U_{ij} = B_{ij}/r_{ij}^{12} - A_{ij}/r_{ij}^{6}$, and a Coulombic term. The A terms in the Lennard–Jones equation were determined from the modified Slater–Kirkwood equation by the method of Pitzer.[19] The equation used was $A_{ij} = [3/2e\hbar/m^{1/2}\alpha_i\alpha_j]/c_{ij}$, where $c_{ij} = (\alpha_i/N_i)^{1/2} + (\alpha_j/N_j)^{1/2}$. The atomic polarizabilities (α) were obtained from data by Ketelaar,[20] and the "effective" number of electrons (N) was estimated by the method of Scott and Scheraga.[21] The B coefficients were calculated by the technique used by Brant, Miller, and Flory[22] which requires the potential to be minimized at the sum of the van der Waals radii (r^0) plus 0.2 Å. The expression was $B_{ij} = A_{ij}(r_j{}^0 + r_j{}^0 + 0.2)^6/2$. Values of r^0 used in this work were obtained from the compilation by Bondi.[23] A tabulation of r^0, α, and N values is given in Table II.

Table II
Parameters Employed in the Potential Calculations

Atom or Group	r^0, Å	α, $\times 10^{24}$ cm^3	N	Q
N	1.55	1.15	6.0	−0.32
P	1.80	2.80	14.1	0.82
O	1.52	0.64	7.0	−0.25
C	1.70	0.93	5.3	0.90 (in CF_3)
H	1.20	0.42	0.9	0.0
F	1.47	0.38	7.9	−0.30
CH_3	2.17	1.95	8.0	0.0
CH_2	1.80	1.77	7.0	0.0
CH (aromatic)	1.77	1.72	6.0	0.0

The Coulombic potential between the atoms i and j as a function of distance (r) was calculated from the expression: $V_{ij} = kQ_iQ_j/\epsilon r_{ij}$. The partial electronic charges (Q) were estimated from electronegativity values by the procedure of Smyth,[24] and these are listed in Table II. It was considered inadvisable to derive these values from quantum mechanical calculations because of the presence of heavy elements, such as phosphorus, in the system. The dielectric constant of all four polymers was estimated to be 3.0. The conversion constant (k) was 332.0, to express the energies in kcal/mol.

It was assumed that no intrinsic torsional potential restricts the torsional mobility of the backbone bonds. This assumption was based on the lack of experimental evidence for such a potential and on the expectation that dπ–pπ bonds in the backbone would generate no significant barrier due to the diffuseness and spherical symmetry of the phosphorus 3d orbital cloud.[6,7]

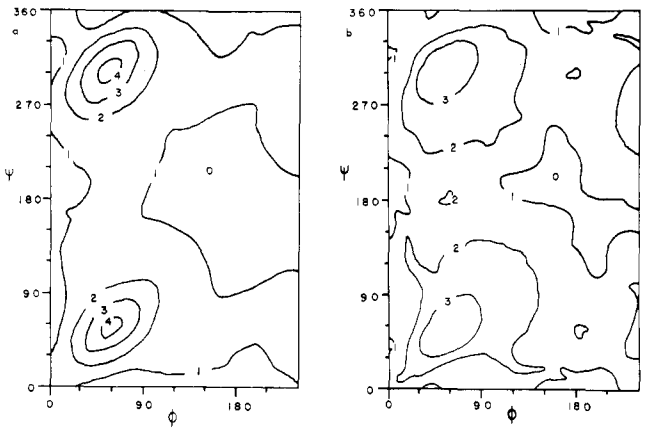

Figure 1. Energy surface calculated for poly(dimethoxyphosphazene), $[NP(OCH_3)_2]_n$. (a) Model A, in which the N–P–N bond angle is 121°. (b) Model B, in which the N–P–N angle is 116.7°.

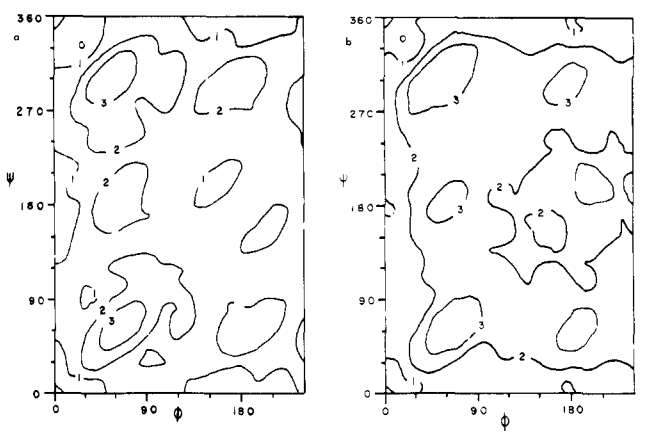

Figure 2. Potential energy surface calculated for poly(diethoxyphosphazene), $[NP(OCH_2CH_3)_2]_n$. (a) Model A, with the terminal methyl groups represented by an "expanded" carbon atom. (b) Model B, with individual hydrogen atoms incorporated into the terminal methyl groups.

The total conformational energy for each interaction was determined by a summation of the nonbonded and Coulombic interaction energies over all atoms in a given conformation, so that the total energy was equal to $\Sigma_{ij}U_{ij} + V_{ij}$. For each *skeletal* conformation, the program scanned all possible side group orientations and selected the energy minimum. The energy surfaces shown in Figures 1–4 represent these side-group minimized potentials and reflect the expected compensatory avoidance motions of the side groups as the skeleton undergoes its conformational changes. A provision in the program allowed the minimum energy conformation of each side group to be ascertained at each skeletal conformation. The interactions between atoms separated by only two bonds were assumed to be invariant with respect to bond torsion. Hence, these energies were not included in the energy summation. The computations were carried out with Fortran IV programs by the use of an IBM 370/168 computer.

Results

The total potential energy values were used to generate conformational energy surfaces for each of the alkoxy- and aryloxyphosphazene polymers. The calculated energy surfaces are shown in Figures 1–4. Figures 1 and 2 are contoured at 1 kcal/mol residue intervals while Figures 3 and 4 are contoured at 2 kcal/mol residue intervals above the absolute energy minimum. The important features obtained from the surfaces

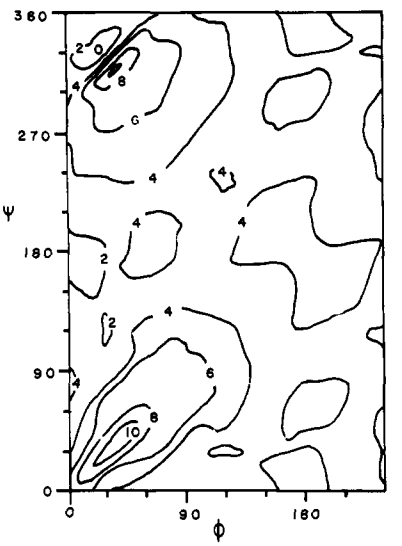

Figure 3. Calculated energy surface for poly[bis(trifluoroethoxy)-phosphazene], $[NP(OCH_2CF_3)_2]$.

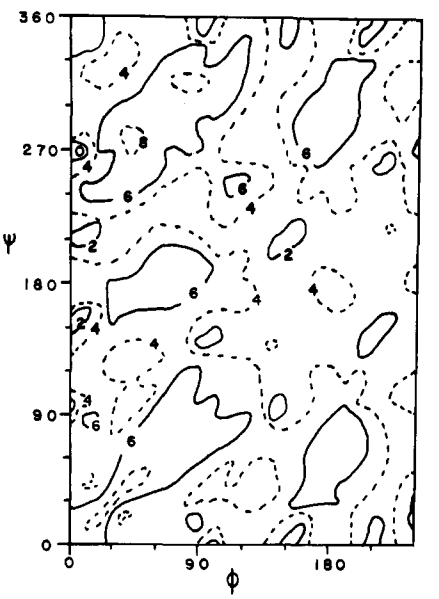

Figure 4. Energy surface for poly(diphenoxyphosphazene), $[NP(OC_6H_5)_2]_n$.

are tabulated in Table III. The barriers listed represent the energy maxima that must be traversed as the backbone bonds undergo 360° torsion. Two energy values are listed. The first is for conformational changes that pass through the absolute energy minimum. The second value represents the barrier to conformational changes that pass through secondary minima. Each polymer is discussed in turn.

$[NP(OCH_3)_2]_n$. The energy surfaces for poly(dimethoxyphosphazene) are shown in Figures 1a and 1b. These two maps differ with respect to the structural input parameters and especially in the N–P–N angle used. Figure 1a represents structural input parameters derived from the cyclic $[NP(OCH_3)_2]_4$, in which the N–P–N angle is 121°. Figure 1b is based on a model with a narrower N–P–N angle of 116.7°, somewhat surprisingly found in the cyclic octamer,[26] $[NP(OCH_3)_2]_8$.

The most striking features of both surfaces are the broad areas of low potential that extend from the region near the cis-cis (ψ = 180°, ϕ = 180°) conformation to the cis-trans (ψ = 0°, ϕ = 180°) conformation. No barriers in excess of 1–2

Table III
Conformational Minima, Barrier Heights, and Minimum Energy Values for Poly(alkoxy- and aryloxyphosphazenes)

	Principal minima,[a] deg	Barriers,[b] kcal/mol residue	Min. energy values, kcal/mol residue
$[NP(OCH_3)_2]_n$-A	160:200	1.26	−25.76
	0:200 (0.32)	0.80	
	0:320 (0.76)		
$[NP(OCH_3)_2]_n$-B	160:200	1.57	−26.54
	0:200 (0.74)	1.12	
	0:320 (0.97)		
$[NP(OCH_2CH_3)_2]_n$-A	30:330	1.11	−32.38
	0:220 (0.66)	1.07	
	160:210 (0.83)		
$[NP(OCH_2CH_3)_2]_n$-B	20:340	1.59	−33.12
	0:180 (0.81)	1.49	
	160:210 (1.52)		
$[NP(OCH_2CF_3)_2]_n$	30:330	3.20	−280.54[c]
	0:180 (0.66)	2.85	(−10.18)
	150:210 (1.19)		
$[NP(OC_6H_5)_2]_n$	10:270	5.21	−43.14
	10:150 (0.99)	2.68	
	150:210 (1.01)		

[a] Torsional angles ϕ and ψ, respectively. The values in parentheses are energy values above the absolute minimum in kcal/mol residue. [b] The first value is for rotation across the energy map through the absolute minimum. The second value is for rotation through the secondary minimum. [c] The larger value is due to a large Coulombic term from the polar CF_3 groups, plus the Lennard–Jones parameter. The second value is from the Lennard–Jones term only.

kcal/residue must be surmounted throughout this region. As might be expected, the narrowing of the N–P–N angle resulted in slightly higher barriers (Table III) and a slight diminution in the breadth of the main low-energy depressions (Figure 1b).

$[NP(OCH_2CH_3)_2]_n$. Figure 2 shows the energy surfaces calculated for poly(diethoxyphosphazene). Model A (Figure 2a) assumed a spherical model for the terminal methyl groups, whereas model B (Figure 2b) included the individual hydrogen atoms of the terminal methyl units. These changes had a small but perceptible influence on the energy surfaces. For model A, the minima appeared at $\psi = 30°, \phi = 330°$; $\psi = 0°, \phi = 220°$; and $\psi = 160°, \phi = 210°$, and in model B the minima were $\psi = 20°, \phi = 340°$; $\psi = 0°, \phi = 180°$; and $\psi = 160°, \phi = 210°$. Model B also generated a slightly lower absolute minimum but raised the barriers by about 0.5 kcal/residue. However, both models generated broad areas of low energy near the cis-cis and cis-trans conformations that were indicative of a high conformational mobility. The similarities between these two surfaces indicated that the spherical methyl group approximation provides a useful approximation for use in complex calculations.

$[NP(OCH_2CF_3)_2]_n$. Although a Coulombic potential was incorporated into the calculations for all four polymers, only for poly[bis(trifluoroethoxy)phosphazene] did this term exert a profound effect. Addition of the electrostatic term to the Lennard–Jones potential caused the absolute energy minimum to drop from −10.18 kcal/mol residue to −280.54 kcal/mol residue. Obviously, this effect can be attributed to the presence of 12 fluorine atoms per residue and to their interactions with the carbon and phosphorus atoms which bear partial positive charges.

However, the magnitude of the Coulombic influence had very little effect on the shape of the surface, or on the positions of the minima. Hence, errors in the partial charge estimates would have very little effect on the conformational predictions. The barrier heights were increased by about 1.5 kcal/residue when the Coulombic term was added. Again, the shape of the energy surface (for combined Lennard–Jones and Coulombic interactions) (Figure 3) revealed broad areas of low potential that could account for a facile backbone torsional mobility in this polymer.

$[NP(OC_6H_5)_2]_n$. Figure 4 shows the energy surface calculated for poly(diphenoxyphosphazene). In contrast to the other three polymers, the model for this derivative generated a surface that contained minima as sharp, restricted depressions in a broad plateau. The restricted minima themselves had energies of less than 2 kcal/mol residue, and these formed the base of rather narrow "canyons" with energies from 2 to 4 kcal/mol residue. Perhaps the most surprising feature of the energy surface for this polymer is the fact that the barriers within the "canyons" are so low (~3 kcal/mol residue). Space filling molecular models of this polymer are almost impossible to construct because of the bulky characteristics of the phenoxy group. However, it is apparent from the calulations that these side groups can undergo subtle avoidance motions as the backbone bonds undergo torsion.

Comparisons of the Four Polymers

Minimum Energy Chain Conformations. Both $[NP(OCH_2CF_3)_2]_n$ and $[NP(OC_6H_5)_2]_n$ readily form microcrystalline phases that yield sharp x-ray diffraction patterns. The repeat distances (~4.9 Å) obtained from the oriented polymers preclude virtually all chain conformations except those close to a cis-trans planar ($\psi = 0°, \phi = 180°$) conformation.[27] The methoxy and ethoxy derivatives have so far failed to yield crystalline-type x-ray patterns. The chain conformation assumed in the crystalline state is usually related to a calculated minimum energy conformation. All four polymers showed pronounced calculated minima at or close to the cis-trans planar conformation (Figures 1–4 and Table III). Although these minima were not the lowest in any surface, they were less than 1 kcal/mol residue above the absolute minimum in each case. Presumably, the combined effects of an extended conformation (for lateral chain packing) and the presence of an intramolecular energy minimum near this point explains the conformations found in the solid state at 25 °C. Thus, *inter*molecular forces may provide additional stabilization for this conformation.

The other conformational minima predicted for $[NP(OCH_2CF_3)_2]_n$ and $[NP(OC_6H_5)_2]_n$ appear to be readily accessible over only moderate barriers. Hence, these minima may be successively occupied at higher temperatures during the known crystal–crystal transitions in these polymers.[14,28] Those minima that are seen close to the cis-cis conformation at $\psi = 150°, \phi = 210°$ may be precluded by the longer-range interactions not incorporated into the model. It should be noted that the lowest calculated minimum for $[NP(OC_6H_5)_2]_n$ (at $\psi = 270°, \phi = 0°$) corresponds to an unusual "step"-type conformation.

It is possible that these low barriers and the unusual breadth of the main energy minima for $[NP(OCH_3)_2]_n$ and $[NP(OC_2H_5)_2]_n$ (Table III, Figures 1 and 2) precludes the adoption of a regular repeating chain conformation and this, in turn, may explain the absence of microcrystalline x-ray diffraction effects.

Minimum Energy Side-Group Conformations. Table IV summarizes the side-group conformations at the chain conformations that represent the main minima. These results provide a starting point for the x-ray structure determination of the polymers.[27]

Chain Flexibility. The flexibility or elasticity of a polymer

Table IV
Side-Group Orientations at Minimum Energy Conformations of the Skeleton and Side Groups

Polymer	Minima[a]	R_1	R_2	R_3	R_4[b]	T_1	T_2	T_3	T_4
$[NP(OCH_3)_2]_n$-A	160:200	C	C	C	C				
	0:200	C	A	C	C				
	0:320	C	B	C	C				
$[NP(OCH_3)_2]_n$-B	160:200	C	C	C	C				
	0:200	C	A	C	C				
	0:320	C	B	C	C				
$[NP(OCH_2CH_3)_2]_n$-A	30:330	C	C	C	C	A	A	A	A
	0:220	C	C	C	C	A	A	A	A
	160:210	C	C	C	C	A	A	A	A
$[NP(OCH_2CH_3)_2]_n$-B	20:340	C	C	C	C	A	A	A	A
	0:180	C	C	C	C	A	A	A	A
	160:210	C	C	C	C	A	A	A	A
$[NP(OCH_2CF_3)_2]_n$	30:330	C	C	C	C	A	A	A	A
	0:180	C	C	C	C	A	A	A	A
	150:210	C	C	C	C	A	A	A	A
$[NP(OC_6H_5)_2]_n$	10:270	A	B	C	B	B	C	C	B
	10:150	A	C	C	C	B	C	C	C
	150:210	C	C	C	C	C	B	C	B

[a] Skeletal torsional angles ϕ and ψ, respectively. [b] Positions A, B, and C are depicted in structures VI and VII. Groups R_2, R_4, T_2, and T_4 are assumed to be represented by mirror images of VI and VII.

is generally believed to be a function of the flexibility of the polymer chains. A low glass transition temperature is an indication of a high chain mobility. High chain flexibility may be a function of two factors: the breadth of the minimum energy wells and the presence of low barriers between the principal wells. Hence, it was of interest to examine the energy surfaces calculated for $[NP(OCH_3)_2]_n$, $[NP(OCH_2CH_3)_2]_n$, and $[NP(OCH_2CF_3)_2]_n$ in a search for clues to the reasons for the low T_g values of these polymers.

The energy surfaces calculated for all three polymers show both broad areas of low potential and low barriers between the main wells. Extensive conformational changes can apparently occur within the wells for all three cases without the surmounting of barriers greater than 1–2 kcal/mol residue. Furthermore, the energy barriers to the transition from one minimum conformation to another are not excessive (<3 kcal/mol residue) for these three alkoxyphosphazene polymers. On the other hand, the surfaces for poly(diphenoxyphosphazene) showed more restricted low-energy areas, with higher barriers (3–5 kcal/mol residue) between conformational minima. Thus, the presumed conformational mobility derived from the energy surfaces, which decreases in the order $[NP(OCH_3)_2]_n \approx NP(OC_2H_5)_2]_n > [NP(OCH_2CF_3)_2]_n \gg [NP(OC_6H_5)_2]_n$, roughly parallels the change in T_g values in the order: −76, −84, −66, and −8 °C. The reversal of the expected order for the methoxy and ethoxy derivatives probably reflects the influence of the longer ethoxy units on reducing intermolecular chain–chain interactions.

Acknowledgment. We thank the Army Research Office for the support of this work.

References and Notes

(1) This paper is part 29 in a series on phosphorus–nitrogen compounds.
(2) Part 28: H. R. Allcock, R. W. Allen, and J. J. Meister, *Macromolecules*, preceding paper in this issue.
(3) H. R. Allcock and R. L. Kugel, *J. Am. Chem. Soc.*, **87**, 4216 (1965).
(4) H. R. Allcock, R. L. Kugel, and K. J. Valan, *Inorg. Chem.*, **5**, 1709 (1966).
(5) H. R. Allcock and G. Y. Moore, *Macromolecules*, **5**, 231 (1972).
(6) H. R. Allcock, "Phosphorus-Nitrogen Compounds", Academic Press, New York, N.Y., 1972.
(7) H. R. Allcock, *Chem. Rev.*, **72**, 315 (1972).
(8) H. R. Allcock, *Chem. Technol.*, **5**, 552 (1975).
(9) D. P. Tate, *J. Polym. Sci., Polym. Symp.*, **No. 48**, 33 (1974).
(10) R. E. Singler, N. S. Schneider, and G. L. Hagnauer, *Polym. Eng. Sci.*, **15**, 321 (1975).
(11) S. H. Rose, *J. Polym. Sci., Part B*, **6**, 837 (1968).
(12) G. S. Kyker and T. A. Antkowiak, *Rubber Chem. Technol.*, **47**, 32 (1974).
(13) H. R. Allcock, R. L. Kugel, and E. G. Stroh, *Inorg. Chem.*, **11**, 1120 (1972).
(14) T. M. Connelly and J. K. Gillham, *J. Appl. Polym. Sci.*, in press.
(15) K. D. Gibson and H. A. Scheraga, *Proc. Natl. Acad. Sci. U.S.A.*, **58**, 420 (1967).
(16) The *A* and *B* parameters for an aromatic CH group were calculated with a polarizability estimated from data by Ketelaar and a van der Waals radius slightly smaller than that proposed for a CH_2 group. The method is analogous to the expanded carbon atom approach for methyl groups.
(17) Reference 6, Appendix I, and ref 7.
(18) F. S. Ezra and R. L. Collin, *Acta Crystallogr., Sect. B*, **29**, 1398 (1973).
(19) K. S. Pitzer, *Adv. Chem. Phys.*, **2**, 59 (1959).
(20) J. Ketelaar, "Chemical Constitution", Elsevier, New York, N.Y., 1958, p 91.
(21) R. A. Scott and H. A. Scheraga, *J. Chem. Phys.*, **42**, 2209 (1965).
(22) D. A. Brant, W. G. Miller, and P. J. Flory, *J. Mol. Biol.*, **23**, 47 (1967).
(23) A. Bondi, *J. Phys. Chem.*, **68**, 441 (1964).
(24) C. P. Smyth, "Dielectric Behavior and Structure", McGraw-Hill, New York, N.Y., 1955, pp 289–311.
(25) G. B. Ansell and G. J. Bullen, *J. Chem. Soc. A*, 2498 (1971).
(26) N. L. Paddock, J. Trotter, and S. H. Whitlow, *J. Chem. Soc. A*, 2227 (1968).
(27) Detailed x-ray analyses of these two polymers are being carried out in our laboratory.
(28) G. Allen, C. J. Lewis, and S. M. Todd, *Polymer*, 11, 44 (1970).
(29) L. E. Sutton, Ed., *Chem. Soc. Spec. Publ.*, **No. 11**, M 128 (1958).
(30) W. C. March and J. Trotter, *J. Chem. Soc. A*, 169 (1971).

Communications to the Editor

Solubility of Hydrogen in Single Crystalline Polyethylene

In a previous research[1] we were able to demonstrate a far higher solubility of hydrogen in single crystalline mats of linear polyethylene (PE) than in ordinary bulk PE. Per gram of sample the hydrogen solubility was fivefold greater in the single crystalline mats than in the bulk PE, but per gram of amorphous phase in which the hydrogen is believed[1] only to dissolve (studies on cyclopropane solubility[2] in PE agreed also with this conclusion) the solubility in the single crystalline mats at 25 °C and 1 atm of pressure of hydrogen was tenfold greater. (Lowell and McCrum[2] did not observe any enhanced solubility of cyclopropane in their single crystal sample as compared to bulk PE.)

Now, however, we have studied hydrogen solubility[3] in some freeze-dried single crystalline samples which became available to us.[4] Much to our surprise no solubility of hydrogen at all could be detected in these rather fluffy crystals although two attempts at 25 °C and one at 35 °C were made to measure the solubility.

Previously,[5] we had thought that the greatly enhanced